Eurasian Chemico-Technological Journal 16 (2014) 179-194

The Importance of Detailed Chemical Mechanisms in Gas Turbine Combustion Simulations

M. Braun-Unkhoff, E. Goos, T. Kathrotia*, T. Kick,
C. Naumann, N. Slavinskaya, U. Riedel

Institute of Combustion Technology, German Aerospace Center (DLR),
Pfaffenwaldring 38-40, 70569 Stuttgart, Germany

Abstract

This paper – in memory of Jürgen Warnatz – summarizes selected recent papers of the Chemical Kinetics Group at the German Aerospace Center in Stuttgart. It shows the need for detailed chemical reaction mechanisms to understand practical combustion systems. A comprehensive description of combustion processes based on detailed mechanisms is especially important in the design of new gas turbine combustion chambers and in the optimization of existing ones to improve efficiency and to reduce pollutant emissions, with fuel-flexibility and load-flexibility ever becoming more important.

Different aspects of combustion processes where detailed reaction mechanisms provide useful insights will be covered in this paper: Fuels (alternative jet fuels, biomass based fuels), pollutants (soot), diagnostics (chemiluminescence), and thermochemistry. Furthermore, the underlying thermodynamics inevitably connected with detailed reaction schemes will be addressed.

Exemplified results will be presented clearly demonstrating the predictive capabilities of detailed reaction mechanisms to be explored in computational fluid dynamic simulations to further optimize technical combustion systems.

Introduction

The late Jürgen Warnatz early recognized the needs for detailed chemical kinetics in reactive flow simulations. Starting in the early 80s, simulating one-dimensional laminar flames, he published numerous well cited papers on detailed chemical kinetics mechanisms for broad class of reactive flows like combustion, hypersonic re-entry flows, and catalytic systems; thus paving the way for predictive computational fluid dynamics simulations.

It is now increasingly recognized that detailed mechanisms are inevitably needed to predict fuel oxidation, pyrolysis, and the formation of pollutants associated with it. This is especially true for gas turbine combustion where a wide range of temperature, pressure, and fuel-air-ratio needs to be covered by the reaction model.

Recently, triggered by the need for increased fuel flexibility, security of supply and reduction of CO_2 as well as pollutants, the use of biogenic gases for stationary power generation and the use of (sustainable) alternative aviation fuels have gained significant interest.

The aim of this paper is to summarize selected recent papers of the Chemical Kinetics Research Group at the German Aerospace Center at Stuttgart to exemplify the role of detailed chemical mechanisms in gas turbine combustion. The combustion chemistry model covers a wide range of temperature, pressure, and fuel-air-ratio to adequately describe the different combustion regimes dominated e.g. by ignition (or re-ignition) or flame propagation and heat release.

A comprehensive description of gas turbine combustion processes based on such detailed mechanisms is especially important in the design of new and in the optimization of existing gas turbine combustion chambers to improve efficiency and to reduce pollutant emissions with fuel-flexibility and load-flexibility ever becoming more important.

* Corresponding author. E-mail: trupti.kathrotia@dlr.de

Fuels

Alternative Jet Fuels

Fossil fuels comprise the largest part of our current energy sources used in electric power generation, transportation, and aviation. However, its limited supply has led to the search of alternative and renewable energy resources. Environment is another issue where renewable energy sources can ensure not only security of supply but also provide an option to combat greenhouse gas emissions.

New concepts require sustainability with respect to feedstock, production, and final product. New production lines based on alternative and more renewable sources have been initiated for more than a decade. For a reliable, efficient, and safe use of new fuels, detailed knowledge on combustion properties is inevitable.

Renewable fuels are already in use for the road transportation sector where natural gas or biogas, ethanol or biodiesel blends reduces the dependence on fossil fuel. Development of fuel flexible and hybrid cars, have provided more flexible usage of new concept fuels. Availability of certified fuels has convinced the buyers, as an example E10 is being used in many countries worldwide as automotive fuel.

The aviation sector has also been part of the increasing efforts on finding alternative fuels. Since decades, only kerosene has been used as jet fuel worldwide [1, 2]. The total consumption of jet fuel was about 5.2 million barrels per day in 2010 [3]. In the current worldwide scenario, jet fuel constitutes 6% of the global oil consumption and about 2% of the total CO_2 emission [4]. If one considers the foreseen annual 5% increase in air traffic, then 2050 will see increase in CO_2 emission by an approximate factor of six [5].

The search for alternative fuels is also induced by policy demands. The current energy policy agreed by the European Commission includes the renewable energy roadmap proposing, among other measures, a binding 20% target for the overall share of renewable energy by 2020. The aviation sector is embedded in this EU policy package concerning renewable energy and CO_2 emissions. In 2011, the European Commission has launched the European Advanced Biofuels Flight Path, an industry wide initiative to speed up the commercialization of aviation biofuels in Europe. The «European Advanced Biofuels Flight Path» initiative is a roadmap with clear milestones to achieve an annual production of two million tons of sustainably produced biofuel for aviation by 2020.

Introducing new fuel for aircraft engines is a great challenge as this requires very strict and specific constraints of various physical and chemical properties such as e.g. freezing point, energy content, boiling point, viscosity, polarity, surface tension, flash point, flammability limit, amount of aromatics, and minimum ignition temperature. Therefore, any new fuel must be compatible to today's engine design. These fuels therefore need to be at least as good as the existing Jet A-1.

Typically, Jet A-1 consists of four chemical families: branched and unbranched alkanes, naphthenes and aromatics. Several investigations have obtained surrogates describing most properties of Jet A-1 including its detailed reaction mechanisms [6–11].

A large variety of feedstock, processes, and resulting products have been discussed so far [5, 9, 12, 13]. Synthetic fuels can be obtained from fossil (coal, gas) and from renewable sources (waste, biomass) by gasification via the Fischer-Tropsch (FT) route. For the midterm outlook, Jet A-1 blended with synthetic paraffinic kerosene (SPK) obtained from a FT-process or hydro treatment is considered to be the most promising option. Among them, BtL (Biomass-to-Liquid), HRJ (Hydrogenated Renewable Jet), and HEFA (Hydro processed Esters and Fatty Acids) are the ones to provide substantial benefits regarding sustainability and CO_2 emissions. In addition, new plant (or vegetable) oils or fatty acids, blended with kerosene can also be a future candidate. Hydrocracking of the vegetable oil can manufacture kerosene and high-quality diesel for which industries are already setting up sites. The modern hydrogenation followed by catalytic conversion provides an important feature where the carbon chain length (short or long molecules) as well as the chemical family of the products (branched or long-chained paraffines) can be influenced. Thereby, the important physical properties of the resulting products such as cetane index and cold flow properties can be controlled according to the required fuel specifications. The renewable synthetic jet fuels known as alcohol to jet (ATJ) and sugar to jet (STJ) are under process of certification by ASTM.

Two fuels based on coal (CtL -Coal-to-Liquid), both developed by SASOL, were the first alternative jet fuels approved for commercial aviation: a semi synthetic jet fuel (SSJF), in 1999, and a fully synthetic jet fuel (FSJF), in 2008 [14] whereas GtL (Gas-to-Liquid) was introduced in 2009. Lufthansa has successfully tested flights operated between Hamburg and Frankfurt, with a bio-derived fuel (50% blend to crude oil kerosene) in one of the two engines of an A321 [15].

Within this context, a detailed reaction model can describe, and, in addition, maybe also predict, major combustion properties e.g. heat release, ignition behavior, and pollutant formation, once vali-

dated by relevant experiments. Thus, the need for running experiments with a particular fuel and for specific parameters (temperature, pressure, fuel-air ratio) can be reduced, saving time and costs. In addition, in some cases, numerical simulations offer the only way to study in detail the influence of the fuel or of specific fuel components on the temperature distribution, the flow field, and pollutant formation in gas turbines for different operating parameters.

Biomass Based Fuels

Fuels derived from low quality feedstock such as biomass and biomass residues have a large potential for power generation, for instance in gas turbines via gasification processes, in micro gas turbines designed for decentralized power generation or combined heat and power, or in Integrated Gasification Combined Cycle plants [16–19]. Improvements on the fuel flexibility of the syngas combustion technology with optimization of the design will widen the acceptable range in the variation of fuel blending and operation conditions. The use of biomass in small, low power facilities offers an efficient, CO_2-neutral and environmental friendly conversion to electrical energy and heat.

Thus, the coupling of thermal gasifiers or biogas reactors with micro gas turbines allows the efficient use of biomass in these facilities. Different feedstocks like algae, wood, sewage sludge, waste, etc. can be used. Micro gas turbines exhibit higher fuel flexibility and substantially lower pollutant emissions compared to conventional gas engines. Therefore, a technically complex and costly exhaust gas treatment can be avoided and a broader range of liquid and gaseous fuels can be used [20]. Moreover, micro gas turbines operate at higher exhaust gas temperatures, thus delivering process heat for further use, e.g. an increase of the electrical efficiency of small gas turbines to more than 50% can be achieved in a hybrid power plant through the combination with a solid oxide fuel cell (SOFC) [21, 22].

The knowledge of fundamental combustion chemistry is important as it provides important information on heat release and auto ignition derived from a simulation with a reaction kinetics model. The fuel flexible gas turbine combustors require knowledge of fundamental properties of the fuel based on reaction kinetics model developed to explain chemistry interactions with turbulent conditions prevailing in the system.

Hence, the overall goal of ongoing research activities is to provide combustion relevant properties of biomass-based gases for a wide range of parameters, creating a sound database for optimized gas turbine design.

Pollutants – Soot

Pollutant formation has been an important topic in many chemical kinetics studies. Soot produces adverse effect on human health, pollutes the environment and can create mechanical failure of the combustion system by forming carbon deposits. Over many years efforts have been attempted to understand the behavior of soot formation in combustion. Soot formation starts from gaseous phase transferring to solid polymer like structures. The transition of gases to liquids or liquids to solid is unclear. In the fuel rich mixtures, C_2-, C_3-precursors lead to the formation of polycyclic aromatic hydrocarbons (PAH) which are precursors itself to the soot formation processes. To produce a reliable model for predictions of soot levels in combustion systems has been a great challenge. Soot modelers face two main problems – the first is to model correctly the PAH gas-phase chemistry that leads to the soot particle nucleation, and the second is to model the particle growth and oxidation in a manner that reflects the physical processes in the flame. The fundamental understanding of PAH growth and particle nucleation leading to soot is still eluding scientific community. Therefore accurate modeling of soot particles from PAH remains an important goal of the combustion community.

Accurate modeling of PAH would require understanding of several interdependent PAH and soot formation processes. Soot inception takes place due to combination of PAHs which further aggregates into larger structures. In another path, soot growth is contributed due to the condensation of PAH on the surface of soot particles.

The soot particle nucleation is assumed to take place due to collision of two pyrene molecules [23, 24]. The most suggested path towards pyrene formation is the hydrogen-abstraction-carbon-addition (HACA) pathway [25, 26] where acetylene addition to benzene leads to pyrene. However, the HACA model does not produce a sufficient amount of pyrene [27, 28]. The prediction of pyrene is seen to be improved when additional pathways towards its formation where used [29, 30].

The aggregation, surface growth, and oxidation follow the soot particle inception in non-premixed flames. Soot particle aggregates are formed from primary spherules [31]. To model this phenomenon, the sectional method [29, 32–34] is one of the approaches used. In this method primary particles are separated on mass basis [35] and then aggregates are divided further according to number of primary particles [36]. In surface growth, it is believed, either condensation of PAH on particles takes place or the growth is following the HACA pathway.

Modeling of soot formation still is a great challenge. To accurately predict soot inception one requires detailed PAH growth mechanism which is difficult to assemble. This is apparent from various studies performed in different groups, by Frenklach [37, 38], D'Anna & Kent et al. [39, 40], Marinov and coworkers [41, 42] and at DLR [23, 26, 30, 43].

Diagnostics – Chemiluminescence

In combustion diagnostics, luminescence occurring due to chemical excitation, referred as chemiluminescence, is very well known. The spontaneous emissions of these lights due to chemical reactions offer an inexpensive diagnostics of flames and combustion processes. Due to its natural self-occurrence, it is non-intrusive to the measurement environment and provides financial benefits by avoiding alternate expensive laser instrumentation.

The four major emitters found in hydrocarbon flames are OH*, CH*, C_2*, and CO_2* [44], where "*" refers to electronically excited state of species. In the emission spectrum, it is found in the visible and ultra-violet (UV) band. Various studies since the early 1970 have identified chemiluminescence as a marker for heat release, reaction zone, and equivalence ratio. Due to its internal occurrence, the chemiluminescence can provide an easy diagnostic option for on-line measurement in combustion applications. The well-known problem of lean combustion in modern combustion applications is that due to its low temperature and lean environment they are subjected to instabilities due to heat release fluctuations. Therefore, for active control one requires sensors that are fast, robust and non-intrusive.

But establishing a correlation between chemiluminescence and these parameters is not an easy task: This requires accurate prediction of the formation and consumption kinetics mechanism of chemiluminescent species. Therefore, a reaction mechanism that precisely predicts the excited species emission is very valuable. Very few studies have focused on the reaction kinetics mechanism that can explain the formation and consumption of these species [45–47]. The excited species are a minor channel of the overall combustion process and are only indirectly linked to the major reaction channels. Therefore the important formation pathways of these species remained under debate until present. For the same reason, experimental determination of reaction rates is also difficult.

As a marker of heat release, several flame observables such as CH, CH_2O, etc. have been studied [48, 49]. Formaldehyde has always been used as an indicator for heat release along with its concentration product with OH [48]. In the narrow flame zone, CH has been found. Likewise chemiluminescent species are also found in the reaction zone [49].

Thermochemistry

Due to the fact that thermodynamical equilibria will normally not reached in combustion systems or practical technical applications, the importance of thermochemical data in process engineering and process optimization, is eminent, too. Thermochemical calculations are important in these design processes, as they provide information if a process can take place, how much energy is needed or will be released [50]. Correct prediction of heat release is important as it influences wall heat load and therefore necessary temperature stability of wall material or of needed efficiency of mostly necessary cooling system, especially in combustion processes. Additionally, thermochemical calculations can predict the energy efficiency of the whole process chain and are therefore an important tool to reduce the consumption of limited resources such as fossil, alternative biomass based or synthetic fuels.

In the development of predictive detailed chemical models, which are used to predict the time dependence and final state of a chemical process, as concentration changes and yields of main and side products, as well as of emissions or undesired substances, which can produce high costs through their need of disposal, reliable thermochemical data are necessary. In most detailed chemical models the reactions are written as reversible reactions. Reactants and products are connected by the temperature and pressure dependent forward reaction rate coefficients. The reaction rate will then be calculated from the actual composition of the mixture and the forward rate coefficient given. Does the reaction also proceed in the backward direction as given in the chemical model then the reaction rate will be calculated using the forward rate and the "equilibrium constant", thus using the thermochemical data, which always has to be provided with the detailed chemical model.

The quality of thermochemical data used influences the quality of reaction rate calculated as well as branching ratio of competing reaction pathways of involved substances. Therefore, it influences the prediction of technical relevant properties as ignition delay times [51], laminar flame speeds and of emissions. To predict correctly pollutant concentrations such as nitrogen oxides and its lower temperature "Prompt NO_x" formation process, thermochemical properties of the highly reactive intermediate NCN [52] play a major role, as it was shown for different hydrocarbon flames with methane and acetylene as fuel.

Thermochemical data of radicals or other highly reactive chemical substances cannot be measured directly. But temperature dependent thermochemical functions such as enthalpy, entropy, Gibbs free energy and heat capacities can be calculated with statistical methods from well-known spectroscopic and molecular properties [53]. Nowadays, using appropriate quantum chemical electronic structure methods [54], molecule specific properties, as rotational constants and vibrational frequencies, can be calculated with high accuracy. Using them, accurate thermochemistry data can be calculated as well, as it was shown for the biradical NCN [52], recently.

The correct prediction of the inhibition of the radical chain propagation during hydrogen ignition and hydrogen oxidation under a wide range of technical relevant conditions [55] as well as the extension of the validation range of detailed syngas (H_2/CO) combustion model to technical relevant high pressure conditions [56] shows that using reliable thermochemical and kinetic data together allows constructing detailed chemical models with predictive behavior over a wide range of conditions in terms of concentration, pressure, and temperature.

But these examples are not limited only to gas phase processes. In recent developed sectional kinetic model for the pyrolysis of cellulose [57], a main component in biomass, the pyrolysis and its combustion products can be described correctly over a wide range of different heating rates.

Also, evaporation and spray formation of liquid fuels during combustion processes depend on thermochemical data (as evaporation enthalpy), as well as phase equilibria between different liquids or of compressible gases such as carbon dioxide or in mixtures with inert gases such as nitrogen [58], which play an important role for transportation of sequestrated carbon dioxide, produced in post combustion processes.

Reaction Kinetics

Fuel Characterization

Alternative Jet Fuels

In the present work, two alternative jet fuels studied earlier are presented, namely GtL (representative of Fischer-Tropsch Synthetic Paraffinic Kerosene (FT-SPK) and CtL (representative of fully synthetic jet fuel (FSJF)) [12]. These fuels contain different chemical families such as branched-, unbranched-paraffinic, naphthenic, and aromatic compounds. The selection of wide chemical families reflects possible options potential fuel could provide in short to long term strategies.

Sasol developed the first FSJF in 2008 for commercial use in aircraft and thereby as a drop-in alternative to kerosene [14]. It is produced from coal applying the FT process, therefore named coal-to-liquid, containing 50% FT-SPK and aromatics derived from severely hydro-treated coal tar kerosene. Since it is produced under controlled condition, it contains a narrow component distribution of several chemical families compared to a wider distribution typically found in Jet A-1 [12, 14]. Compared to CtL, GtL was chosen representing FT-SPK which meets SPK specifications [59] and contains less than 0.5% aromatics. Further a blend of GtL with 50% naphthenic compounds intended to bring the FT-SPK blend into Jet A-1 specification limit [59] and a blend with 20% oxygenated compound to get the benefit of reduced emission has been discussed by [9].

To model the described fuels, surrogates are formulated. A detailed GS-MS analysis is performed on the GtL and CtL fuels provided by Sasol. This analysis showed that the GtL can be best represented by a mixture of *n*-decane, iso-octane, and *n*-propylcyclohexane whereas CtL surrogate consists of a four component mixture n-decane, iso-octane, propylcyclohexane, and *n*-propylbenzene. The reaction mechanism used for modeling both fuels' oxidations consists of 8217 reactions and 2185 species [60].

The laminar burning velocity measurements are performed for GtL-, GtL-surrogate- and Jet A-1-air flames at atmospheric condition. These measurements are compared in Fig. 1 with the flame speed of the GtL surrogate with a mixture composition of 57.7 mol % *n*-decane, 33.2 mol % iso-octane, and 9.1 mol % *n*-propylcyclohexane determined in GC-analysis discussed earlier. The flames studied are at pre-heat temperature of 473 K and fuel stoichiometry varies from 1.0 to 1.5. The suitability of the selected surrogate is evident from the figure where the measured GtL data agree within 5% with the mixture prepared from the GtL-surrogate. It should be noted that the stoichiometric range of the measurement is restricted from about 1.0 to 1.5 due to the limitations of our measurement technique where the flame beyond this range is either extinguished (lean condition) or is unstable (rich condition) which adds to the difficulty in obtaining burning velocity by the cone angle method [9]. A very good agreement is seen between our measurement and simulation. The GtL measurement of present work agrees with the spherical expanding flames of Vukadinovic et al. [61]. Similarly, Fig. 2 shows data for a CtL-air mixture consisting of (39.5 mol % *n*-decane, 13.0 mol % iso-octane, 10.2 mol % *n*-propylbenzene, and 37.3 mol % *n*-propylcyclohexane) along with Jet A-1. The simulated flame speed is

slightly lower than the measured ones in between φ = 1.0 to 1.05. The simulations are in reasonable well agreement with the measurements. As the GtL and CtL burning velocities are very similar to the Jet A-1 velocities, both alternative fuels are similar to Jet A-1 with respect to the laminar flame speed.

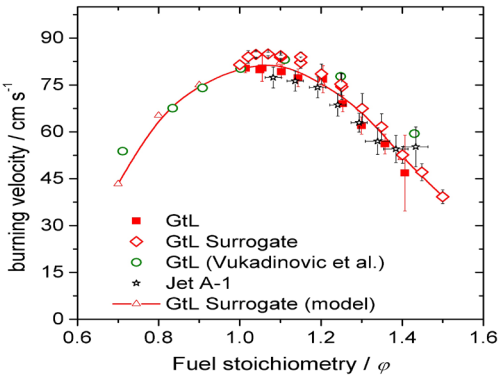

Fig. 1. Measured burning velocity and simulated flame speed of GtL, GtL-surrogate, and Jet A-1 mixtures. Conditions: T_0 = 473 K, p = 1 bar.

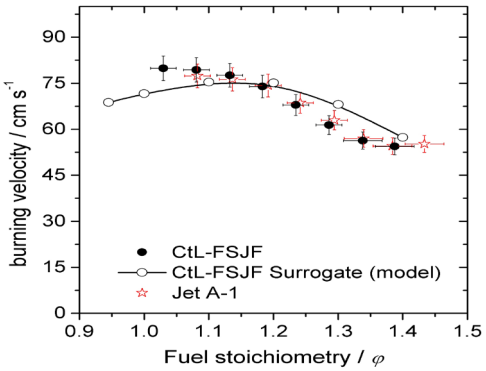

Fig. 2. Measured burning velocity and simulated flame speed of CtL and Jet A-1 mixtures. Conditions: T_0 = 473 K, p = 1 bar.

Ignition delay times of GtL and CtL fuel mixtures were measured in a high pressure shock tube with an internal diameter of 46 mm. The features of the setup are described elsewhere [9, 62]. In addition to both alternative fuels, their respective surrogates were also measured. Fuels and synthetic air (20% O_2 / 80% N_2) mixtures (dilution of 1:2, with nitrogen) were prepared in two different fuel stoichiometries φ = 0.5 and 1.0 and ignition times were determined at pressure of about 16 bar. The ignition was followed by CH* emission profiles observed at 431 nm and the criteria for ignition delay times were obtained from the difference between reflected shock front and peak CH* emission. The simulations were done with the above stated surrogates and reaction mechanism using the Multiple Plug Flow Reactor (MPFR) code – an DLR Stuttgart extension of Chemkin II [63–65]. In Figs. 3 and 4, ignition delay times of measured alternative fuels (GtL, CtL), their surrogates, and Jet A-1 mixtures are shown. The modeled fuel-surrogate mixture is denoted by the solid line. For both fuel stoichiometry studied, the ignition delay times of all the three mixtures are very close to each other. A small difference in Jet A-1 mixture is seen at temperatures lower than 1100 K. Here, the temperature dependence within the NTC region is not well reproduced by the simulations.

These studies have also shown that addition of naphthenes (*n*-propylcyclohexane), and aromatics (*n*-propylbenzene) to *n*-alkane have minor influence on fundamental combustion properties.

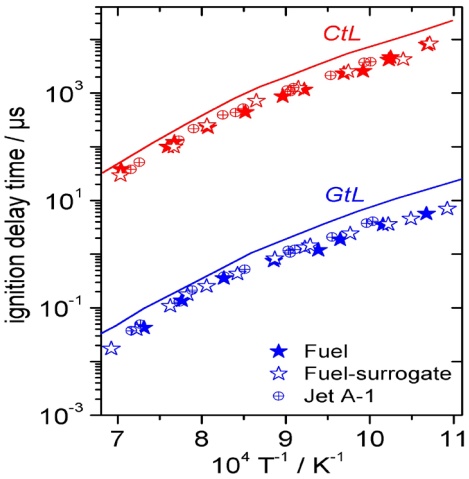

Fig. 3. Measured and computed comparison of ignition delay time of GtL and CtL fuels at φ = 0.5, p = 16 bar. Lines are simulations of stated fuel-surrogate with pressure profile.

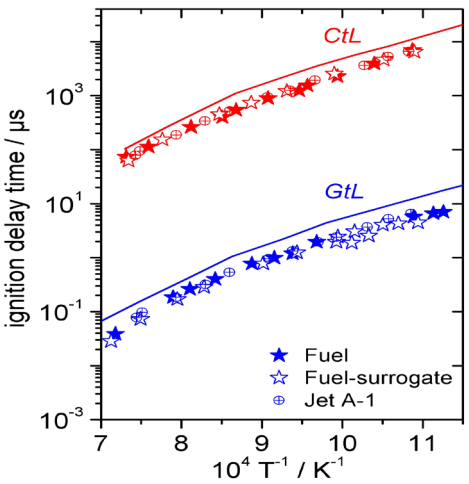

Fig. 4. Measured and computed comparison of ignition delay time of GtL and CtL fuels at φ = 1.0, p = 16 bar. Lines are simulations of stated fuel-surrogate with pressure profile.

Fuels from Biomass

The development of fuel flexible gas turbine combustors with low emission characteristics and high reliability requires validated chemical kinetic reaction models, as they are one of the essentials among a variety of models and methods used in Computational Fluid Dynamics (CFD) simulations. Hence, experimental data sets on fundamental combustion properties as laminar flame speeds and auto ignition delay times of biomass-derived gases for a wide range of parameters supports the improvement and validation of reaction mechanism used within the combustor design process.

For this purpose, experiments on the laminar flame speed S_u and on the ignition delay times τ of gasification products of two different feedstocks (Table 1) – from the gasification products of wood and the fermentation products of algae [66] – were performed at conditions typical for so called "micro gas turbine combustors". The data for S_u and τ were compared with the predictions of different reaction models, among them the reaction model of Li et al. [67] shown here.

Table 1

Composition of the gas mixtures considered: Product gases from gasification of wood and of fermentation of algae [66] and gas mixtures used for validation experiments.

Species	Wood gasification			Algae fermentation		
	Product gas I	Mixture I to measure τ and S_u		Product gas II	Mixture II, to measure τ and S_u	
CH_4	0.025	0.051	0.068	0.52	1	1
CO_2	0.127	0.258	-	0.28	-	-
N_2	0.508	-	-	0.15	-	-
CO	0.186	0.378	0.510	-	-	-
H_2	0.154	0.313	0.422	-	-	-

The ignition delay times were measured in a stainless steel shock tube with an inner diameter of 10 cm behind the reflected shock front near the end plate. Pressure transducers along the axis and emission detection of OH* and/or CH*, resp., were recorded to calculate shock conditions and to monitor auto ignition. By definition, ignition delay time was defined as the time difference between the initialization of the reaction system and the maximum of OH*- or CH*-emission recorded.

Laminar flame speed measurements were performed according to the cone angle method using contraction nozzles of different contraction ratios depending on the flame speed. Calibrated mass flow controllers were used for mixture preparation and co-flow adjustment. Flame emission, spectrally filtered and intensified, if required, was recorded through a CCD-camera, and digitally filtered to gain the cone-angle.

Comparisons of the data with H_2, H_2/CO, reference gas (92% CH_4, 8% C_2H_6), and CH_4 ignition delay times are presented in Fig. 5. The temperature dependence of the data of the wood gasification product is very similar to those of H_2 and H_2/CO. Therefore, it is concluded that the chemistry is determined by the H_2 content, the CH_4 at this concentration level causes only a slight increase of ignition delay times as CO_2 does by its chaperon efficiency, too. Not only becomes this increase stronger with higher CH_4 content, but also the characteristic increase of the apparent activation energy typical for hydrogen dominated reaction systems changes drastically [65]. Reaction model predictions for the laminar flame speed measurements of mixture I from wood gasification are shown in Fig. 6.

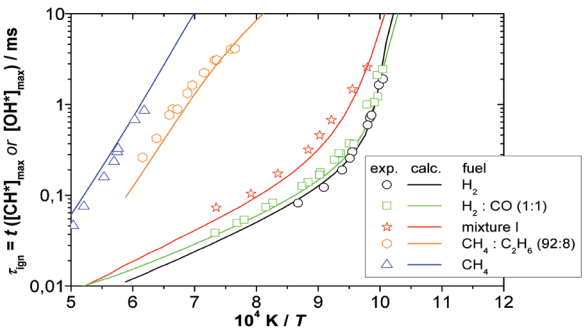

Fig. 5. Measured and calculated ignition delay times of different fuels at stoichiometric conditions and a pressure of 4 bar, diluted 1:5 in Argon; oxidizer: 79% Ar, 21% O_2. Lines: simulations based on the mechanism of Li et al. [67]. Black: H_2 [65], green: 50 vol% H_2/50 vol% CO [68], red: mixture I, orange: reference gas (natural gas) [68], blue: CH_4 [69].

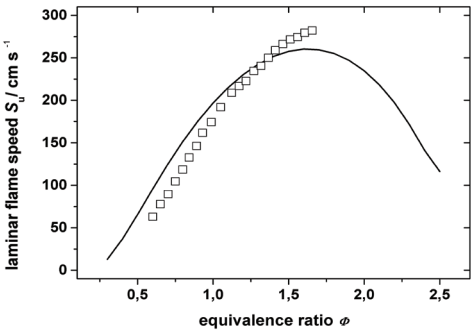

Fig. 6. Measured and calculated laminar flame speed for mixture I at ambient pressure and at preheat temperature of 473 K; oxidizer: synthetic air (80% N_2, 20% O_2). Solid line: simulations based on the mechanism of Li et al. [67].

Auto ignition delay times as well as burning velocities of hydrogen / hydrogen rich fuels and methane / natural gas differ significantly. Hence, mixtures of hydrogen with natural gas as well as hydrogen rich biogenic gases containing carbon monoxide and/or methane cover a wide range of ignition delay times and burning velocities and therefore pose high demands on a reaction models predictive capability.

Soot Prediction

In order to accurately model soot formation in combustion simulation algorithms, numerous chemical/physical mechanisms which contribute to overall soot concentration need to be considered. These include polycyclic aromatic hydrocarbon (PAH) growth/particle inception, surface growth via surface chemistry and via PAH condensation, surface oxidation, particle coagulation and fragmentation, gas phase scrubbing, and radiation. The soot particle inception depends on local concentrations of aromatic species, the size of which depend on the fuel being burned. Hence, the detailed and accurate chemical kinetics mechanism of PAH growth are necessary if accurate simulation of soot formation in inception-dominated combustion regimes are desired. Slavinskaya and Frank [30] proposed a mechanism for C_1 and C_2 fuel combustion and PAH growth up to five-ring aromatics, with further improvement recently in [27, 28, 70]. The mechanism of PAH formation was deduced with the aim of describing the formation of aromatics up to C_{20} and their radicals, which have been detected in non-negligible concentrations in flame experiments involving CH_4, C_2H_4, and C_2H_6. These species are benzene (A1), toluene (C_7H_8), phenylacetylene ($A1C_2H$), styrene ($A1C_2H_3$), indene (C_9H_8), naphthalene (A2), biphenyl, (P2), acenaphthylene (A2R5), phenanthrene (A3), pyrene (A4), benzo(ghi)-fluoranthene, (BGHIF), chrysene ($C_{18}H_{12}$), benzo(a)py-rene, (BAPYR), and some of their branched structures and radicals, see Table 2.

The reaction paths for aromatic species production have been assembled by analyzing the data reported in the literature over the last thirty years. All reasonably well-established routes from small aliphatic molecules to first aromatic rings and pre-particle molecular weight growth were considered: HACA mechanism, hydrogen atom migration yielding five- and six-member rings, inter-conversion of five- and six-member rings and zigzag aromatic edges, resonantly stabilized free radical addition schemes, methyl substitution/acetylene addition pathways, cyclopentadienyl moiety in aromatic ring formation, and reactions between aromatic radicals and molecules. The small radicals CH_3, C_2H, C_2H_3, H_2CCCH, C_3H_4, C_4H, H_2CCCCH, C_4H_5, C_5H_5 and small molecules C_2H_2, C_4H_2, C_4H_4, C_6H_2 were used as "building blocks" for PAH molecule growth and for H-atom abstraction from hydrocarbons. Hydrogen atom migration was considered as part of the HACA reaction set. The resulting mechanism was tested against 23 experimental data sets obtained for laminar premixed CH_4 and C_2H_4 flames at atmospheric pressure, in shock tube experiments under elevated pressure, and in coflow ethylene/air diffusion flames. The model successively reproduces all considered experimental sets. Some examples of the model predictive capabilities are shown in Figs. 7-9.

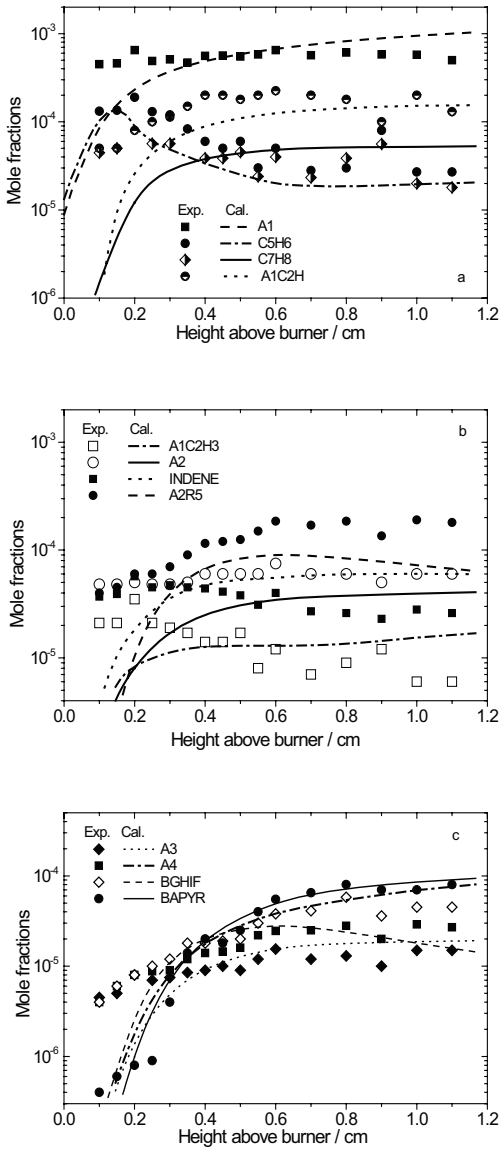

Fig. 7. Aromatics in the laminar atmospheric $C_2H_4/O_2/Ar$ flame, φ = 3.06. Symbols – experimental data [71, 41]; lines – calculations.

Table 2
Nomenclature of aromatic species

Name	Structure	Graph	Name	Structure	Graph
Phenyl, A1-	C_6H_5		Methylnaphthalene, A_2CH_3	$C_{11}H_{10}$	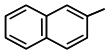
Benzene, A1	C_6H_6		Ethynylnaphthalene, A_2C_2H	$C_{12}H_8$	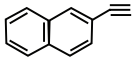
Toluene	C_7H_8		Acenaphthalene, A2R5	$C_{12}H_8$	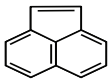
Benzyl, C_7H_7	$C_6H_5CH_2$		Phenanthrene, A3	$C_{14}H_{10}$	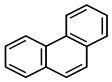
Phenyl acetylene, $A1C_2H$	$C_6H_5C_2H$	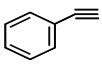	Methylphenanthrene	$C_{14}H_{12}$	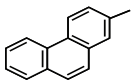
Ethynylphenyl radical, $A1C_2H$-	C_6H_4CCH	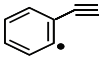	Phenanthrylacetylene $A3C_2H$	$C_{16}H_{10}$	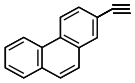
Styrene, $A1C_2H_3$	$C_6H_5C_2H_3$	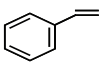	Pyrene, A4	$C_{16}H_{10}$	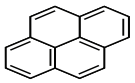
Phenylvinyl radical, $A1C_2H_3$*	$C_6H_4CH=CH_2$	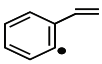	Pyrene acetylene, $A4C_2H$	$C_{18}H_{10}$	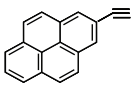
n-Styryl, *n*-C_8H_7	$C_6H_5CH=CH$	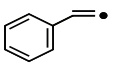	Benzo(ghi)-fluoranthene, BGHIF	$C_{18}H_{10}$	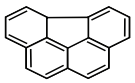
Indene	C_9H_8	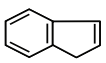	Chrysene	$C_{18}H_{12}$	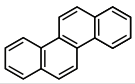
Naphthalene, A2	$C_{10}H_8$	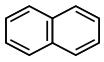	Benzo(a)pyrene, BAPYR	$C_{20}H_{12}$	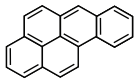
Biphenyl, P2	$C_{12}H_{10}$	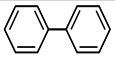			

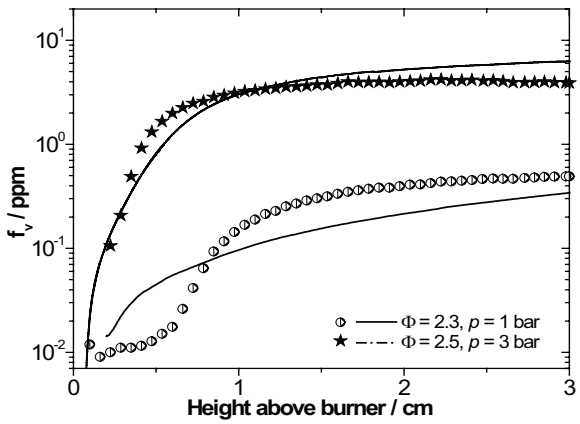

Fig. 8. Calculated and measured soot volume fractions f_v for the laminar atmospheric C_2H_4/air flame: p = 1 bar, φ = 2.3 and p = 3 bar, φ = 2.5. Symbols – experimental data [72]; lines – calculations.

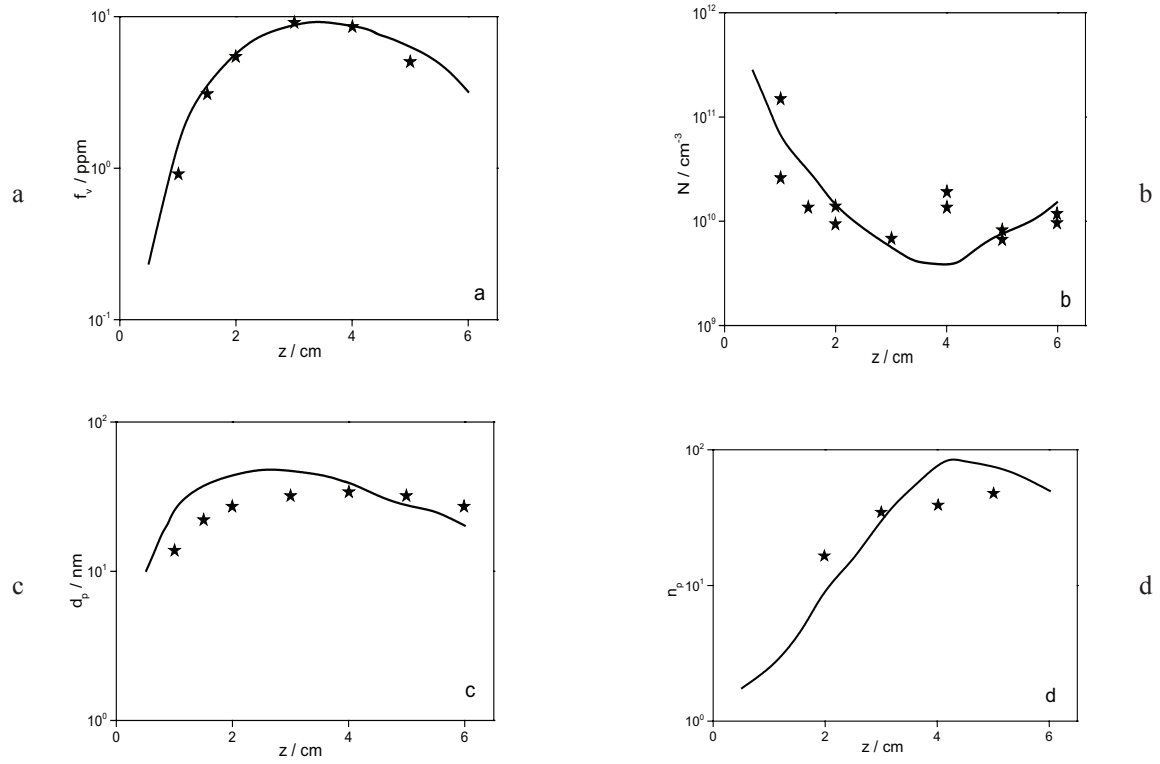

Fig. 9. Comparison of calculations [27] with experiments: a) soot volume fraction, b) particle number density, c) average primary particle diameter, and d) average number of primary particles per aggregate. Measured data have been obtained in diffusion co-flow flames for a) [73], b) [74], c) [75], and d) [76].

Chemiluminescence as Heat Release Marker

Chemiluminescence species are seen to be formed from intermediate species such as CH, C_2H, C_2, C_3, etc. found in reaction zones [47]. The concentrations of excited species are very low compared to their precursors. Therefore, unreliability in precursor's concentration may directly translate into uncertainty in chemiluminescence prediction. The reaction mechanisms which are tuned to predict global parameters such as flame speed and ignition delay or even flame product or intermediate species other than immediate precursors of chemiluminescent species may not be adequate. Additional difficulties in mechanism development arise when the reaction channel responsible for excited species formation cannot be directly evaluated [47]. This is evident from the large scatter seen in the reaction rate predictions by different studies in literature [46].

The precursor species from which chemiluminescent species are formed are mainly found in the reaction zone. Therefore, the peak intensities of chemiluminescent species appear in reaction zone. The displacement between the appearances of the maximum of excited species and species mainly found in the reaction zone will provide information on chemiluminescence as reaction zone marker. Various studies have focused to correlate and characterize the reaction zone with chemiluminescence [48, 77, 78]. In addition, efforts have been made to understand if chemiluminescene can be identified as a marker for heat release [48, 78, 79]. They have shown that the maximum intensities of excited species are found close to the location of where the heat release peaks. As an example, in Kathrotia et al., [47], we have shown that in a CH_4-air flame, at different fuel equivalence ratios (φ = 0.5–1.6) the location of OH* and CH_2O appearance is found closest to the heat release location. Among other chemiluminescent species, CH* followed OH* and the most deviation from heat release was found with C_2*. This trend remained unaffected by fuel stoichiometry. This numerical experiment was done at 298 K initial temperature and pressure of one bar in a laminar flat flame. Under the condition studied and considering the resolution of the measurement techniques (few millimeters for this laboratory flame), the OH* and CH* represent a good marker for the heat release location compared to C_2* which appears much farther.

Our mechanism predicting OH*, CH*, and C_2* kinetics published earlier in Kathrotia et al., [47] has

been used to calculate three CH_4-, C_2H_4-, C_2H_6-air premixed laminar flames. The results of these flames were evaluated and ratios of maximum heat release rate to maximum excited species mole fraction were obtained. As shown in Fig. 10, the ratio of the maximum heat release to the maximum mole fraction of an excited species is plotted against equivalence ratios. These ratios are obtained for all above three flames studied.

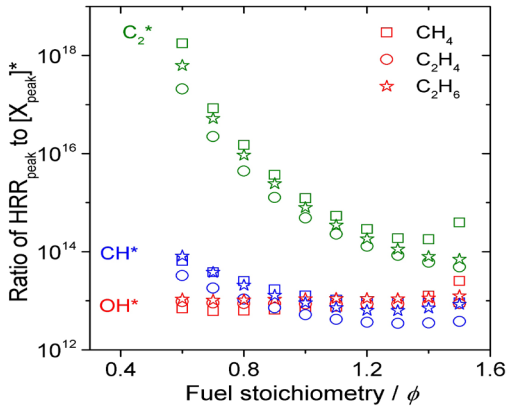

Fig. 10. Comparison of the ratio of heat release rate to ratio of peak concentration of chemiluminescent species (OH*, CH*, C_2*) at different fuel stoichiometry and for three different flames (CH_4-, C_2H_4-, C_2H_6-air). The calculations are performed for 298 K initial temperature and at atmospheric pressure.

It is seen that the ratio shows little dependence on fuel type considered in this study. In addition, for OH* and CH*, it remained independent of fuel stoichiometry. Only in the case of C_2*, the ratio shows decreasing behavior with increasing fuel stoichiometry however the trend remains same for all three fuels. This shows that chemiluminescence can be correlated to the heat release rate and a given system can be calibrated to obtain various combustion parameters such as equivalence ratio.

The present numerical study is only limited to laminar flame condition. It should be noted that the laser measurements provides better spatial and temporal resolution compared to chemiluminescence in turbulent flames. However, future studies in turbulent systems can provide more insight into the potential of chemiluminescence as a marker for heat release and reaction zone.

Thermochemistry

Nitrogen Oxide emissions (NO_x) from combustion are regulated by European and also worldwide laws. Prompt NO formation at lower temperatures is an important topic in combustion chemistry, especially related to burner concepts such as FLOX®, which avoid high temperatures and therefore the often dominant thermal NO formation process.

Prompt NO formation was first reported more than thirty years ago by Fenimore [80]. Details about this formation process remained controversial until now. Observed nitrogen oxide (NO) concentrations close to a burner surface in hydrocarbon flames were attributed by Fenimore [80] to reactions forming N-containing intermediates and involving molecular nitrogen and free radicals of hydrocarbons, as potential sources of NO formation.

But spin–orbit coupling in the suggested reaction CH + N_2 => HCN + N was, as theoretical studies [81, 82] showed, not strong enough to account for experimental observations regarding prompt NO formation. Many consecutive studies provided evidence that their suggested alternative product channel CH + N_2 => NCN + H with additional reactions accounted better for the experimental results reported at that time.

From experimental, theoretical, and modeling perspectives two central issue emerged, namely the value of the temperature and pressure dependent rate coefficient of the reaction CH + N_2 => NCN +H in the temperature range around 1500 K – important for technical applications– and the unknown thermochemical data of the involved highly reactive substance cyanonitrene (NCN).

Extensive high level quantum chemical and theoretical kinetic study by Harding et al. [83] on calculation of the reaction rate constant of CH+N_2 => NCN +H solved one central aspect of NCN reaction kinetics. Their results agreed quantitatively with experimental results obtained in shock tubes [84].

Considering the endothermicity of the reaction CH+N_2 => NCN +H it is obvious, that heat of formation for NCN is a highly sensitive quantity in modeling predictions, too, when the NCN pathway for prompt NO formation is implemented in reaction mechanisms. Additionally a more accurate knowledge of the heat of formation of NCN would significantly reduce the remaining uncertainty of Harding et al.´s predictions of the reaction rate coefficient below 2000 K.

Previously reported values for the heat of formation of NCN at 298.15 K differ by more than 50 kJ/mol and the relevance and extent of this uncertainty on model predictions had not been systematically addressed [52] and references therein. This gap was closed through our work [52], where new much more accurate thermochemistry data of NCN with an uncertainty of ± 2.0 kJ/mol was provided.

Temperature-dependent enthalpy increment, heat capacity, and entropy of NCN can be calculated reasonably well, because the influence of uncertainties

in molecular properties of NCN is small in comparison to inconsistencies in the values for heat of formation of NCN at standard conditions.

Indirect experimental determined heat of formation values as well as quantum chemical results on different level of theory differ significantly and are mostly exclusive in the sense that their reported uncertainties do not provide a convincing overlap between the alternatives. Own quantum chemical calculations on different levels of theory gave insight in the reasons for the differences in the values obtained and were used to judge the quality of the results available in literature, as well as to check assumptions made in the indirect experimental determinations.

Finally the Active Thermochemical Table (ATcT) Approach [85, 86] was used to successfully arbitrating between inconsistent values by exploiting redundant thermochemical cycles in the Thermochemical Network (TN), providing that the body of thermochemical-relevant data is sufficiently rich. The TN includes experimental determinations of electron affinity measurements, determinations of N–CN bond dissociation energy and N_2 elimination energy to triplet and singlet carbon as well as calculated total atomization and ionisation energy and isomerisation energies between different isomers.

The analysis exposed some weaknesses of the experimental data (results are significantly less accurate than believed) as well as of single-reference computations, which suffer from spin contaminations. On the other hand analysis of a localized thermochemical network with Active Thermochemical Table showed that the high level multi reference quantum chemical investigations of Harding et al. [83] are remarkably mutually consistent with all reaction energies and reproduce correctly (within 1.7 kJ/mol) doublet–quartet splitting in the CH radical and reaction enthalpy of the reaction CH + N_2 => HCN + N, which are both independent of NCN. The ATcT result from localized thermochemical network using the best available data results in a standard heat of formation of NCN at 298.15 K of 457.8 ± 2.0 kJ/mol, and represents the best currently available thermochemical value, which leads to a consistent picture from a state of the art theoretical perspective. This enthalpy of formation is within the error bars of earlier theoretical multi reference quantum chemical result of Martin et al. [87] and refines it substantially, though it does not longer fully support the experimental result of Bise et al. [88]. These NCN thermochemical data can be downloaded in an easy to use format for modeling with CFD programs as supplementary material from [89].

Additionally the influence of the route via the NCN radical on NO formation in flames was examined from a thermochemistry and reaction kinetics perspective.

For simulating NO formation a validated hydrocarbon oxidation mechanism, which maps the complete set of combustion features as ignition delay times, flame speeds, speciation in reactors, and flames, was extended with best known reaction rates for NCN pathway and new thermochemistry for NCN species included, and the thermochemistry of the other species were updated [90].

In all flames the NCN thermochemistry applied highly influences NO and NCN concentrations simulated. Figure 11 shows the most sensitive reactions for NO and NCN formation within the NO_x chemistry sub model. The surprising result is that not only absolute sensitivities differ significantly (NCN and NO sensitivities) but also the ranking of sensitive reactions changes.

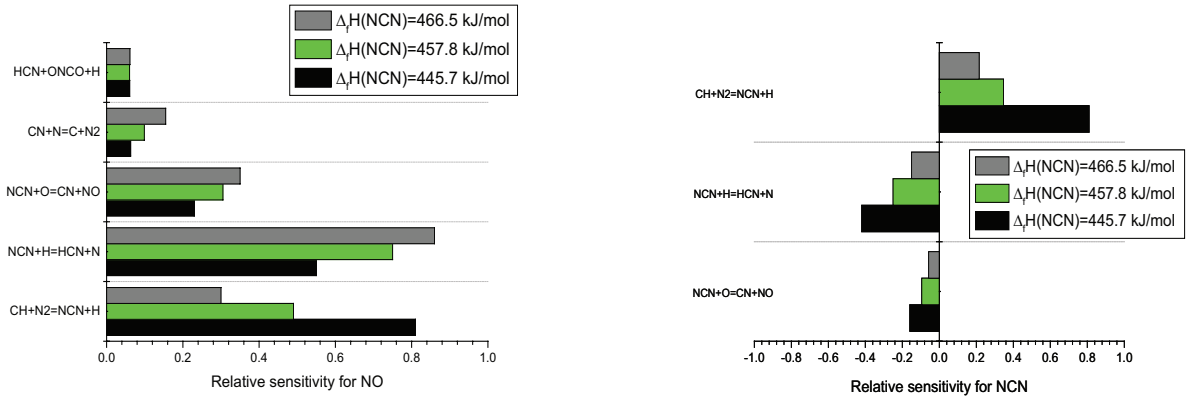

Fig. 11. Relative reaction sensitivity coefficients for mole fractions of NO (upper panel) and NCN (lower panel) of a low pressure laminar methane flame [91] in dependence of different heat of formation of NCN used. All other modeling parameters as well as detailed reaction mechanism, molecular transport properties, and other thermochemical data were unchanged [52]. Most sensitive reaction in the NCN case is $C_2H_3 = C_2H_2 + H$ and in NO case it is $O_2 + H = OH + O$.

The results illustrate thermochemistry constraints in the context of NCN chemistry which have to be taken into account for improving model predictions of NO concentrations in flames and more general for improving model predictions for NO_x emissions in technical applications. Also the results indicate that model predictions for NO concentrations in flames and therefore the prediction of NO_x emissions remain empirical unless the recommended highly accurate heat of formation of NCN is used.

Conclusions

A detailed chemical kinetic model is an essential building block for predictive CFD simulations of turbulent combustion systems, e.g. gas turbine combustors. The search for alternative fuels has lead to new designer fuels consisting of components of various chemical families ranging from branched, unbranched, and cyclic hydrocarbon compounds-available from FT-processes, from biomass gasification, or fermentation. These new fuels have to be tested for physical and chemical properties to get information on its suitability to be used in existing engines designs. An example of CtL, GtL fuels and wood, algae derived gases studied predicting laminar flame speed and ignition delay times has been presented here. The chemical kinetic model development supplies important information on the heat release and ignition delay times and provides chemistry models to predict combustion in CFD simulations.

The prediction of pollutant is also an important part of combustion research as the use of new or existing fuels, due to the strict environmental regulations imposed by many countries, requires compliance with emission limits. In this context, soot has been studied since decades in combustion research and still the understanding of many pathways in its formation chemistry, from gaseous phase to solid particles, remains unclear. An understanding of PAH formation is the key part of the soot inception process for which several literature studies are dedicated. A detailed reaction mechanism including all possible established routes to soot formation has been investigated and a validated mechanism is summarized in this study.

An accurate mechanism cannot be drawn based based on just correct pathways and well predicted rate coefficients. The availability of accurate thermochemistry data also plays an important role in the overall reaction mechanism development. Uncertainties in thermochemistry can lead to erroneous prediction of global combustion behavior as ignition delay times, as well as to erroneous prediction of species concentrations, an example is shown in this study. Thermochemistry is involved in all research and technologies, where chemical reactions are taking place or where knowledge on the energy balance of certain processes is critical. It can be used for optimization of fuel usage (in general raw materials usage) and for management and avoidance of unwanted products.

Many practical combustion applications, including gas turbines, operate under fuel-lean and moderate to low temperatures. At such conditions, instabilities of combustors subjected to heat release fluctuations are high. Therefore an active control of such unstable regimes requires sensors that are fast, robust, and non-intrusive in nature. Chemiluminescene has been identified as a promising alternative to the conventional laser techniques in diagnostics. The numerical study presented here and in literature [47, 48, 78, 79] has shown that various flame observables such as peak species concentrations, heat release rate, and the location of maximum species concentrations can be related to equivalence ratio and correlations can be obtained. Although the environment studied in the present work (laminar conditions) differs from those of practical systems (turbulent conditions), CFD studies at a wide range of conditions (fuels, stoichiometries, and pressure) in real combustors, with chemiluminescence chemistry available from a reliable reaction kinetic mechanism, will provide a better understanding of chemiluminescence as an inexpensive diagnostic tool for process control.

The use of validated detailed reaction mechanism, accurate thermochemical and transport data within CFD modeling studies will increasingly give engineers guidelines for the design, optimization, and improvement of technical highly relevant processes, like combustion, pyrolysis, or gasification.

Acknowledgment

The work on alternative jet fuel was performed within the EU FP7 project ALFA- BIRD: EUFP7/2007-2013, grant agreement no. 213266.

Fuel from biomass research was partly funded by the Stiftung Energieforschung Baden-Württemberg within the project “Entwicklung und Validierung von Design-Werkzeugen für die Auslegung von dezentralen Biomasse-Kraftwerkskonzepten zur kombinierten Strom- und Wärmeerzeugung (DedeBio)“ under contract number FZK A 283 09.

The groups of Prof. Murray J. Thomson (University of Toronto) and Dr. Seth B. Dworkin (Ryerson University Toronto), are gratefully acknowledged for an ongoing fruitful cooperation, and useful discussion leading to the further development of the PAH mechanism.

Financial support for chemiluminescence study from the Deutsche Forschungsgemeinschaft (German Research Foundation, DFG grant no. RI 839/4-2, "Chemiluminescence and Heat Release") is gratefully acknowledged.

Parts of the work on thermochemistry were supported by the COST Action CM0901 "Detailed chemical kinetic models for cleaner combustion".

Thank you for everything Jürgen (U. R.).

References

[1]. P. Dagaut, M. Cathonnet, Prog. Energ. Combust. 32 (2006) 48–92.
[2]. J. Hileman, R. Stratton, P. Donohoo, J. Propul. Power 26 (2010) 1184–1195.
[3]. U.S. Energy Information Administration, http://www.eia.gov.
[4]. IPPC Intergovernmental Panel on Climate Change, 2007:"Climate Change 2007: Mitigation of Climate Change", http://www.ipcc.ch/publications_and_data/publications_ipcc_fourth_assessment_report_ wg3_report_mitigation_of_climate_change.htm.
[5]. M. Braun-Unkhoff, P. Le Clercq, M. Aigner, Proc. 17th European Biomass Conference, Hamburg, Germany (2009).
[6]. M. Braun-Unkhoff, P. Frank, A. El Bakali, A. Ristori, P. Dagaut, M. Cathonnet, A Detailed Kinetic Reaction Mechanism for Kerosene Oxidation at Atmospheric Pressure. 16th International Symposium on Gas Kinetics, Cambridge, UK (2000).
[7]. P. Dagaut, Phys. Chem. Chem. Phys. 4 (2002) 2079–2094.
[8]. Th. Kick, T. Kathrotia, M. Braun-Unkhoff, U. Riedel, Proceedings of GT2011, ASME Turbo Expo, Vancouver (Canada), GT2011-45606
[9]. Th. Kick, J. Herbst, T. Kathrotia, J. Marquetand, M. Braun-Unkhoff, C. Naumann, U. Riedel, Energy 43 (2012) 111–123.
[10]. N. Slavinskaya, Proc. 46th AIAA Aerospace Sciences Meeting and Exhibit, Reno (USA) (2008) Paper no. 0992.
[11]. N. Slavinskaya, A. Zizin, M. Aigner, Proceedings of GT2009, ASME Turbo Expo, Orlando (USA), GT2009-60012.
[12]. ALFA-BIRD: Alternative Fuels and Biofuels for Aircraft, EUFP7/2007-2013, grant agreement # 213266, coordinator: EU-VRi, (Germany), http://www.alfa-bird.eu-vri.eu
[13]. S. Blakey, L. Rye, C. Wilson, Proc. Combust. Inst. 33 (2011) 2863–2885.
[14]. C. Moses, P. Roets, Proceedings of GT2008, ASME Turbo Expo, Berlin (Germany), GT2008-50845.
[15]. burn-FAIR (2011) http://presse.lufthansa.com/en/newsreleases/singleview/archive/2010/november/29/ article/1828.html.
[16]. S. Gadde, J. Wu, A. Gulati, G. McQuiggan, B. Koestlin, B. Prade, Proceedings of GT2006, ASME Turbo Expo, Orlando (USA), GT2006-90970.
[17]. E. Lindfeldt, M. Westermark, Proceedings of GT2006, ASME Turbo Expo, Orlando (USA), GT2006-90183.
[18]. F. Delattin, S. Bram, J. De Ruyck, Proceedings of GT2006, ASME Turbo Expo, Orlando (USA), GT2006-90012.
[19]. M. Braun-Unkhoff, N. Slavinskaya, M. Aigner, Proceedings of GT2009, ASME Turbo Expo, Orlando (USA), GT2009-60214.
[20]. T. Panne, A. Widenhorn, M. Aigner, M. Masgrau, Proceedings of GT2009, ASME Turbo Expo, Orlando (USA), GT2009-59048.
[21]. M. Hohloch, A. Widenhorn, D. Lebküchner, T. Panne, M. Aigner, Proceedings of GT2008, ASME Turbo Expo, Berlin (Germany), GT2008-50443.
[22]. T. Methling, M. Braun-Unkhoff, U. Riedel, Proc. of GT2013, ASME Turbo Expo, San Antonio (USA), GT2013-64994.
[23]. M. Braun-Unkhoff, A. Chrysostomou, P. Frank, E. Gutheil, R. Lückerath, W. Stricker, Proc. Combust. Inst. 27 (1998) 329–336.
[24]. J. Appel, H. Bockhorn, M. Frenklach, Combust. Flame 121 (2000) 122–136.
[25]. H. Wang, M. Frenklach, Combust. Flame 110 (1997) 173–221.
[26]. D. Hu, M. Braun-Unkhoff, P. Frank, Combust. Sci. Technol. 149 (1999) 79–94.
[27]. S. Dworkin, Q. Zhang, M. Thomson, N. Slavinskaya, U. Riedel, Combust. Flame 158 (2011) 1682–1695.
[28]. N. Slavinskaya, U. Riedel, S. Dworkin, M. Thomson, Combust. Flame 159 (2012) 979–995.
[29]. H. Richter, M. Braun-Unkhoff, S. Granata, J. Yu, E. Goos, N. Slavinskaya, P. Frank and W. Green, J. Howard, Proc. European Combustion Meeting ECM 2005, Louvain-la-Neuve, 3.-6. April 2005, paper 163.
[30]. N. Slavinskaya, P. Frank, Combust. Flame 156 (2009) 1705–1722.
[31]. M. Domenico, P. Gerlinger, M. Aigner, Combust. Flame 157 (2010) 246–258.
[32]. F. Gelbard, J. Seinfeld, J. Colloid Interface Sci. 78 (1980) 485–501.
[33]. F. Gelbard, Y. Tambour, J. Seinfeld, J. Colloid Interface Sci. 76 (1980) 541–556.
[34]. J. Marquetand, M. Fischer, I. Naydenova, U. Riedel, Flow and Combustion in Advanced

Gas Turbine Combustors, Fluid Mechanics and Its Applications Fluid Mechanics and its Application, Ed. R. Moreau, Springer (2013) 205–233.
[35]. S. Dworkin, M. Smooke, V. Giovangigli, Proc. Combust. Inst. 32 (2009) 1165–1172.
[36]. M. Saffaripour, P. Zabeti, S. Dworkin, Q. Zhang, H. Guo, F. Liu, G. Smallwood, M. Thomson, Proc. Combust. Inst. 33 (2011) 601–608.
[37]. M. Frenklach, H. Wang, Proc. Combust. Inst. 23 (1990) 1559–1566.
[38]. M. Frenklach, Proc. Combust. Inst. 26 (1996) 2285–2293.
[39]. A. D'Anna, J. Kent, Combust. Flame 121 (2000) 575–592.
[40]. A. D'Anna, J. Kent, R. Santoro, Combust. Sci. Technol. 179 (2007) 355–369.
[41]. N. Marinov, W. Pitz, C. Westbrook, M. Castaldi, S. Senkan, Combust. Sci. Technol. 116 (1996) 211–287.
[42]. N. Marinov, W. Pitz, C. Westbrook, A. Vincitore, M. Castaldi, S. Senkan, Combust. Flame 114 (1998) 192–213.
[43]. M. Kamphus, K. Kohse-Höinghaus, M. Braun-Unkhoff, Combust. Flame 152 (2008) 28–59.
[44]. A.G. Gaydon "The spectroscopy of flames" (1974) Wiley: New York.
[45]. G. Smith, J. Luque, C. Park, J. Jeffries, D. Crosley, Combust. Flame 131 (2002) 59–69.
[46]. T. Kathrotia, M. Fikri, M. Bozkurt, M. Hartmann, U. Riedel, C. Schulz, Combust. Flame 157 (2010) 1261–1273.
[47]. T. Kathrotia, U. Riedel, A. Seipel, K. Moshammer, A. Brockhinke, Appl. Phys. B 107 (2012) 571–584.
[48]. H. Najm, P. Paul, C. Mueller, P. Wyckoff, Combust. Flame 113 (1998) 312–332.
[49]. C. Vagelopoulos, J. Frank, Proc. Combust. Inst. 30 (2005) 241–249.
[50]. E. Goos, A. Burcat, Thermochemistry, in "Handbook of Combustion" M. Lackner, F. Winter, A.K. Agarwal (Eds.), 1 (2010) 135–152.
[51]. L. León, E. Goos, C. Klauer, L. Seidel, F. Mauss, T. Zeuch, Proc. 24th Int. Colloquium on the Dynamics of Explosions and Reactive Systems (ICDERS 2013), July 28 August 2, 2013 Taipei, Taiwan ICDERS-0259, Combust. Flame, to be submitted (2014).
[52]. E. Goos, C. Sickfeld, F. Mauß, L. Seidel, B. Ruscic, A. Burcat, T. Zeuch, Proc. Combust. Inst. 34 (2013) 657–666.
[53]. E. Goos, A. Burcat, "Overview of Thermochemistry and its Application to Reaction Kinetics" H. DaCosta, M. Fan (Eds.), John Wiley & Sons (2011) 3–32. http://media.wiley.com/product_data/excerpt/08/04705823/0470582308-186.pdf
[54]. E. Goos, G. Lendvay, Calculation of molecular chemical data and its availability in databases in "Development of detailed chemical kinetic models for cleaner combustion" F. Battin-Leclerc, J. Simmie, E. Blurock (Eds.), Series: Green Energy and Technology, Springer-Verlag London (2013) 515–547.
[55]. G. Dixon-Lewis, P. Marshall, B. Ruscic, A. Burcat, E. Goos, A. Cuoci, A. Frassoldati, T. Faravelli, P. Glarborg, Combust. Flame 159 (2012) 528–540.
[56]. X. You, H. Wang, E. Goos, C. Sung, S. Klippenstein, J. Phys. Chem. A 111 (2007) 4031–4042.
[57]. T. Lin, E. Goos, U. Riedel, Fuel Process. Technology 115 (2013) 246–253.
[58]. E. Goos, U. Riedel, L. Zhao, L. Blum, Energy Procedia 4 (2011) 3778–3785.
[59]. ASTM D7655, addendum to ASTM Standard D1655 "ASTM D7566 is a new specification for certifying a 50% blend of Jet A-1 and SPK produced from biomass using a Fischer Tropsch process" www.astm.org.
[60]. A. Mze-Ahmed, P. Dagaut, K. Hadj-Ali, G. Dayma, T. Kick, J. Herbst, T. Kathrotia, M. Braun-Unkhoff, J. Herzler, C. Naumann, U. Riedel, Energy & Fuels, 26, 6070-6079.
[61]. V. Vukadinovic, P. Habisreuther, N. Zarzalis, Proceedings of GT2012, ASME Turbo Expo, Copenhagen (Denmark), GT2012-69449.
[62]. P. Dagaut, F. Karsenty, G. Dayma, P. Diévart, K. Hadj-Ali, A. Mze-Ahmed, M. Braun-Unkhoff, J. Herzler, T. Kathrotia, T. Kick, C. Naumann, U. Riedel, L. Thomas, Combust. Flame 161 (2014) 835–847.
[63]. A. Lutz, R. Kee, J. Miller, SAND87-8248, Sandia National Laboratories: Livermore, CA (1987).
[64]. R. Kee, F. Rupley, J. A. Miller, SAND89-8009, Sandia National Laboratories: Livermore, CA (1989).
[65]. J. Herzler, C. Naumann, Proc. Combust. Inst. 32 (2009) 213–220.
[66]. "Entwicklung und Validierung von Design-Werkzeugen für die Auslegung von dezentralen Biomasse-Kraftwerkskonzepten zur kombinierten Strom- und Wärmeerzeugung (DedeBio)", project funded by Stiftung Energieforschung Baden-Württemberg, under contract number FZK A 283 09.
[67]. J. Li, Z. Zhao, A. Kazakov, M. Chaos, F. Dryer, J. Jr. Scire, Int. J. Chem. Kinet. 39 (2007) 109–136, http://www.princeton.edu/

mae/people/faculty/dryer/homepage/kinetic_models/c1-model/
[68]. J. Herzler, C. Naumann, Comb. Sci. Technol. 180 (2008) 2015–2028.
[69]. J. Herzler, J. Herbst, Th. Kick, C. Naumann, M. Braun-Unkhoff, U. Riedel, Proceedings of GT2012, ASME Turbo Expo, Copenhagen (Denmark), GT2012-69282.
[70]. V. Chernov, M. Thomson, S. Dworkin, N. Slavinskaya, U. Riedel, Combust. Flame 161 (2014) 592–601.
[71]. M. Castaldi, N. Marinov, C. Melius, J. Huang, S. Senkan, W. Pitz, C. Westbrook, Proc. Combust. Inst. 26 (1996) 693–702.
[72]. M. Tsurikov, K. Geigle, V. Krüger Y. Schneider-Kühnle, W. Stricker, R. Lückerath, R. Hadef, M. Aigner, Combust. Sci. Technol. 177 (2005) 1835–1862.
[73]. R. Puri, T. Richardson, R. Santoro, R. Dobbins, Combust. Flame 92 (1993) 320–333.
[74]. R. Santoro, T. Yeh, J. Horvath, H. Semerjian, Combust. Sci. Technol. 53 (1987) 89–115.
[75]. C. Megaridis, R. Dobbins, Combust. Sci. Technol. 66 (1989) 1–16.
[76]. S. Iyer, T. Litzinger, S. Lee, R. Santoro, Combust. Flame 149 (2007) 206–216.
[77]. J. Kojima, Y. Ikeda, T. Nakajima, Proc. Combust. Inst. 28 (2000)1757–1764.
[78]. C. Panoutsos, Y. Hardalupas, A. Taylor, Combust. Flame 156 (2009) 273–291.
[79]. T. Kathrotia, U. Riedel, J. Warnatz, 4th Euro. Combust. Meet. Vienna (2009) paper no. P809002.
[80]. C. Fenimore, Proc. Combust. Inst. 13 (1971) 373– 380.
[81]. L. Cui, K. Morokuma, J. Bowman, S. Klippenstein, J. Chem. Phys. 110 (1999) 9469–9482.
[82]. L. Moskaleva, M. Lin, Proc. Combust. Inst. 28 (2000) 2393–2401.
[83]. L. Harding, S. Klippenstein, J. Miller, J. Phys. Chem. A 112 (2008) 522–532.
[84]. V. Vasudevan, R. Hanson, C. Bowman, D. Golden, D. Davidson, J. Phys. Chem. A 111 (2007) 11818–11830.
[85]. B. Ruscic, R. Pinzon, M. Morton, G. von Laszevski, S. Bittner, S. Nijsure, K. Amin, M. Minkoff, A. Wagner, J. Phys. Chem. A 108 (2004) 9979–9997.
[86]. B. Ruscic, R. Pinzon, G. von Laszewski, D. Kodeboyina, A. Burcat, D. Leahy, D. Montoya, A. Wagner, J. Phys.Conf. Ser. 16 (2005) 561–570.
[87]. J. Martin, P. Taylor, J. Francois, R. Gijbels, Chem. Phys. Lett. 226 (1994) 475–483.
[88]. R. Bise, H. Choi, D. Neumark, J. Chem. Phys. 111 (1999) 4923–4932.
[89]. http://dx.doi.org/10.1016/j.proci.2012.06.128
[90]. E. Goos, A. Burcat, B. Ruscic, "Extended Third Millennium Ideal Gas and Condensed Phase Thermochemical Database for Combustion with updates from Active Thermochemical Tables"; available at http://burcat.technion.ac.il/dir, also directly available from Dr. Elke Goos.
[91]. N. Lamoureux, P. Desgroux, A. El Bakali, J. Pauwels, Combust. Flame 157 (2010) 1929–1941.

Received 18 March 2014